THE ASTROPHYSICAL JOURNAL, 324:279–287, 1988 January 1

THE RELATIONSHIP BETWEEN THE EDDINGTON LIMIT, THE OBSERVED UPPER LUMINOSITY LIMIT FOR MASSIVE STARS, AND THE LUMINOUS BLUE VARIABLES

HENNY J. G. L. M. LAMERS[1] AND EDWARD L. FITZPATRICK
Joint Institute for Laboratory Astrophysics, University of Colorado, and National Bureau of Standards
Received 1986 December 10; accepted 1987 June 19

ABSTRACT

The location of the Eddington limit in the temperature-gravity diagram for early-type stars is estimated on the basis of new low-gravity, plane-parallel, LTE model atmosphere calculations, which include the effects of metal line opacity in the Balmer continuum. The observed luminosity upper limit for stars in the Milky Way and the LMC, transformed into a temperature-gravity relation, agrees very well with the predicted Eddington limit for stars with $T_{\rm eff} > \sim 10{,}000$ K. This result suggests that the reversal in the redward evolution of stars as they approach the observed luminosity limit is due to enhanced mass loss in the stars as they naturally evolve toward very low effective gravities.

The kink in the observed luminosity limit near $T_{\rm eff} \approx 10^4$ K and the constant upper limit of $\log L/L_\odot \approx 5.7$ for stars with $T_{\rm eff} < \sim 10^4$ K is due to the fact that the Eddington luminosity reaches a minimum near $T_{\rm eff} \approx 10^4$ K. Stars with a luminosity of $\log L/L_\odot < \sim 5.7$ after their core hydrogen burning phase can continue their horizontal evolution in the HR diagram to the red supergiant phase.

The high mass-loss rates of the luminous blue variables (LBV) during quiescence and their location in the HR diagram (to the left of the upper luminosity limit) can be explained by the fact that the Eddington limit shifts to the left in the HR diagram when a star's mass decreases (due to mass loss) but its luminosity remains constant. The violent outbursts of LBVs are probably due to a conflict between the natural tendency of the stars to expand after the core hydrogen burning phase and the Eddington limit, which requires a shrinking of the star as the mass decreases. Several observational and theoretical arguments support this hypothesis.

Subject headings: stars: atmospheres — stars: interiors — stars: massive — stars: mass loss

I. INTRODUCTION

The upper limit for the luminosity of early-type stars in our Galaxy and in other galaxies of the Local Group is observed to decrease with decreasing effective temperature (Humphreys and Davidson 1979; Humphreys 1987). This so-called Humphreys-Davidson limit (HD limit), as originally defined, runs from $\sim \log (L/L_\odot) = 6.8$ at $T_{\rm eff} = 40{,}000$ K to $\log (L/L_\odot) = 5.8$ at $T_{\rm eff} \approx 15{,}000$ K and remains constant at $\log (L/L_\odot) \approx 5.8$ for cooler stars. This observed upper limit is considerably lower than the classical Eddington limit for electron scattering which lies at $\log (L_{\rm E}/L_\odot) = 7.14$ [assuming the mass-luminosity (M-L) relation for zero-age main-sequence (ZAMS) stars of $40 < M < 120\ M_\odot$ calculated by Maeder (1983, 1987) and extrapolating to higher masses].

The observed $T_{\rm eff}$-dependent luminosity limit implies that the most massive stars, those with an initial mass $M_i \geq \sim 40\ M_\odot$, do not reach the red supergiant phase after core hydrogen burning, but that their almost horizontal evolutionary tracks in the HR diagram turn back toward the left before crossing the HD limit. This behavior can be understood if the fraction of the total stellar mass contained in the He-C-O core reaches a critical value as the stars evolve near the HD limit (Chiosi, Nasi, and Sreenivasan 1978; Maeder 1983). This critical mass fraction is ~ 0.67 for stars with an initial mass $M_i \gtrsim 60\ M_\odot$ and 0.77 for stars with $M_i = 30\ M_\odot$.

The mass-loss rates of normal stars are insufficient to produce such large core mass fractions as the evolutionary tracks approach the HD limit (e.g., Chiosi *et al.* 1978). It has been shown by a number of investigators, however, that combining normal mass-loss rates with enhanced internal mixing, in the form of turbulent diffusion or convective core overshooting, or both, leads to the quasi-homogeneous evolution (i.e., in the direction of the He main sequence) of stars more massive than $M_i > \sim 40\ M_\odot$ (e.g., Maeder 1982; Doom 1982; Pylyser, Doom, and de Loore 1985; Prantzos *et al.* 1986).

Alternatively, it can be assumed that stars nearing the HD limit experience very high mass-loss rates, sufficient to increase the core mass fraction and halt the redward evolution, independently of internal mixing schemes (Maeder 1983). This scenario is supported by observations which show that many stars near the HD limit indeed suffer very large mass-loss rates, on the order of 10^{-5} to $10^{-4}\ M_\odot\ {\rm yr}^{-1}$, suggesting that the high mass-loss rate phenomenon is closely associated with the HD limit. The most prominent examples of those stars are the luminous blue variables (LBVs; Conti 1984), which include the P Cygni type stars in our Galaxy, the S Dor stars in the Large Magellanic Cloud and the Hubble-Sandage variables in M31 and M33.

In this paper we compare the observed upper luminosity limit in the Milky Way and the LMC with the Eddington limit as estimated for plane-parallel LTE model atmospheres, *which include the full effects of metal line opacities in the ultraviolet.* We will show that the HD limit corresponds to the locus of extremely low effective gravities. This result suggests that stars approaching the HD limit will suffer high mass-loss rates because of the reduction of the effective gravity due to radiation pressure. These high mass-loss rates ultimately lead to

[1] On leave from the SRON Laboratory for Space Research and Sonnenborgh Observatory, Utrecht.

the core mass fraction reaching its critical value and the reversal of the stellar evolution tracks. We will show that radiation pressure, as an agent for producing enhanced mass loss near the HD limit, can in a natural way explain the kink in the HD limit near $T_{\rm eff} \approx 10^4$ K and the upper luminosity limit for yellow and red supergiants. We will also discuss the high mass-loss rates of the LBVs, their location in the HR diagram and their evolutionary stage.

II. LOCATION OF THE UPPER LUMINOSITY LIMIT IN THE HR DIAGRAM AND IN THE TEMPERATURE-GRAVITY DIAGRAM

a) The HR Diagram

The HD limit in the HR diagram, as originally defined by Humphreys and Davidson (1979), consists of two linear parts:

$$\log (L/L_\odot) \approx 5.42 + 2.34 \log (T_{\rm eff}/10^4) \quad \text{for} \quad 15{,}000 \leq T_{\rm eff} \leq 30{,}000 \text{ K} ; \quad (1a)$$

$$\log (L/L_\odot) \approx 5.80 \quad \text{for} \quad 3000 \leq T_{\rm eff} \leq 15{,}000 \text{ K} . \quad (1b)$$

Humphreys and Davidson (1979) found that the same limit applies to the Galaxy and the LMC (assuming a LMC distance modulus of 18.6 mag).

A revised luminosity upper limit for Galactic stars was given by Humphreys and Davidson (1984) and adopted in a recent review paper by Humphreys (1987):

$$\log (L/L_\odot) = 5.93 + 0.75 \log (T_{\rm eff}/10^4) \quad \text{for} \quad 5800 \lesssim T_{\rm eff} \lesssim 30{,}000 \text{ K} \quad (2a)$$

$$\log (L/L_\odot) = 5.75 \quad \text{for} \quad T_{\rm eff} < 5800 \text{ K} . \quad (2b)$$

The main refinements in this version of the upper limit include the use of a more recent spectral type—effective temperature calibration and the exclusion of the star η Carinae. The steep slope in equation (1a) is largely due to η Car, whose adopted $T_{\rm eff}$ is that of the optically thick circumstellar matter rather than the photosphere.

It is possible that the revised limit is slightly too high, especially in the $T_{\rm eff}$-dependent parts, because some of the stars near the limit may be in an active phase and suffering enhanced mass loss. During such a phase of shell ejection a star makes a horizontal excursion in the HR diagram (Wolf, Appenzeller, and Cassatella 1980) which results in an underestimate of the effective temperature which the stars would have at quiescence and thus in an overestimate of the luminosity-temperature relation.

Recently, Garmany, Conti, and Massey (1987) have redetermined the upper luminosity limit for stars in the LMC, excluding the "abnormal stars" such as the LBVs. They found an upper limit of

$$\log (L/L_\odot) = 5.71 + 1.22 \log (T_{\rm eff}/10^4) \quad \text{for} \quad 10{,}000 \lesssim T_{\rm eff} \lesssim 40{,}000 \text{ K} . \quad (3a)$$

Garmany *et al.* did not determine the location of the kink in the luminosity upper limit. However, by taking the luminosity limit of the red supergiants as derived by Humphreys (eq. [2b]) and scaling it to the distance modulus of 18.3 mag adopted by Garmany *et al.*, we find that equation (3a) reaches this limit at $T_{\rm eff} = 8600$ K. This results in an estimate of the horizontal part of the HD limit for the LMC

$$\log (L/L_\odot) = 5.63 \quad \text{for} \quad T_{\rm eff} \leq 8600 . \quad (3b)$$

In Figure 1*a* we show the luminosity upper limits of equations (1)–(3), plotted in a temperature-luminosity diagram. Because these lines are upper limits and because the HR diagrams from which they are derived are not densely populated, the statistical significance of the individual relations is difficult to assess. Our aim in showing three different estimates is to indicate the likely level of observational uncertainty in the location of the upper luminosity limit.

b) The $\log T_{\rm eff} - \log g$ *Diagram*

In order to compare the observed upper luminosity limits with the Eddington limits derived in the following section from model atmospheres, we need to convert the $\log T_{\rm eff} - \log L$ relations of equations (1)–(3) into $\log T_{\rm eff} - \log g$ relations. This requires a knowledge of stellar mass (or stellar radius) as a function of luminosity, for which we turn to stellar evolution calculations.

For this study we adopt the *M-L* relation for stars after the core hydrogen burning (CHB) phase, i.e., when the stars start to move to the right in the HR diagram. Evolution calculations have shown that the luminosity remains constant during this expansion phase, and that this phase is so short ($\sim 10^4$ yr for a 60 $M_\odot$ star) that the additional mass loss is negligible. So the *M-L* ratio at the end of the CHB phase is valid until the stars reach the HD limit.

We examined the post–CHB *M-L* relations from evolution calculations by Chiosi *et al.* (1978; the $\alpha = 0.83$ case), by Maeder (1983, 1987) and by Prantzos *et al.* (1986). These calculations all assumed a heavy element abundance of $Z = 0.02$, incorporate the effects of mass loss (although with differing mass-loss rate parametrization schemes), and, for the Prantzos *et al.* and Maeder models, include some form of enhanced internal mixing. Figure 2 shows that, in the range $5.0 \leq \log L/L_\odot \leq 6.5$, the shapes of the three relations are very similar, although they differ by scale factors. At this point we have no compelling reason for choosing any one set of calculations over the others. Therefore, we have fit a simple regression line (taking $\log L/L_\odot$ as the independent variable) through the models shown in Figure 2 over the range $5.2 \leq \log L/L_\odot \leq 6.4$. The result is shown as the dashed line in Figure 2 and can be expressed as a function of mass by

$$\log L/L_\odot = 2.43 + 2.13 \log M/M_\odot . \quad (4)$$

This linear relation satisfactorily represents the shapes of the various *M-L* relations over the luminosity range of interest here ($\log L/L_\odot > \sim 5.5$).

In Figure 1*b* we show the three upper luminosity limits converted into $\log T_{\rm eff} - \log g$ relations using equation (4). The $\log T_{\rm eff}$, $\log L/L_\odot$, $\log M/M_\odot$, and $\log g$ values for all the data in Figure 1 are given in Table 1.

Observationally, the location of the upper limit is well defined in the $\log T_{\rm eff}$–$\log g$ plane. However, a significant potential source of certainty arises from the transformation of luminosity to gravity through the *M-L* relation. We adopt ± 0.1 dex as the uncertainty in the $\log g$ values due to this transformation, as estimated directly from the spread of the various models around the adopted *M-L* relation in Figure 2.

III. THE EDDINGTON LIMIT

a) The Eddington Limit in the HR Diagram and the $\log T_{\rm eff}$*–log g Diagram*

The Eddington limit for instability against radiation pressure is defined by the condition

$$L_{\rm E} = \frac{4\pi G c M}{\kappa_{\rm F}} , \quad (5)$$

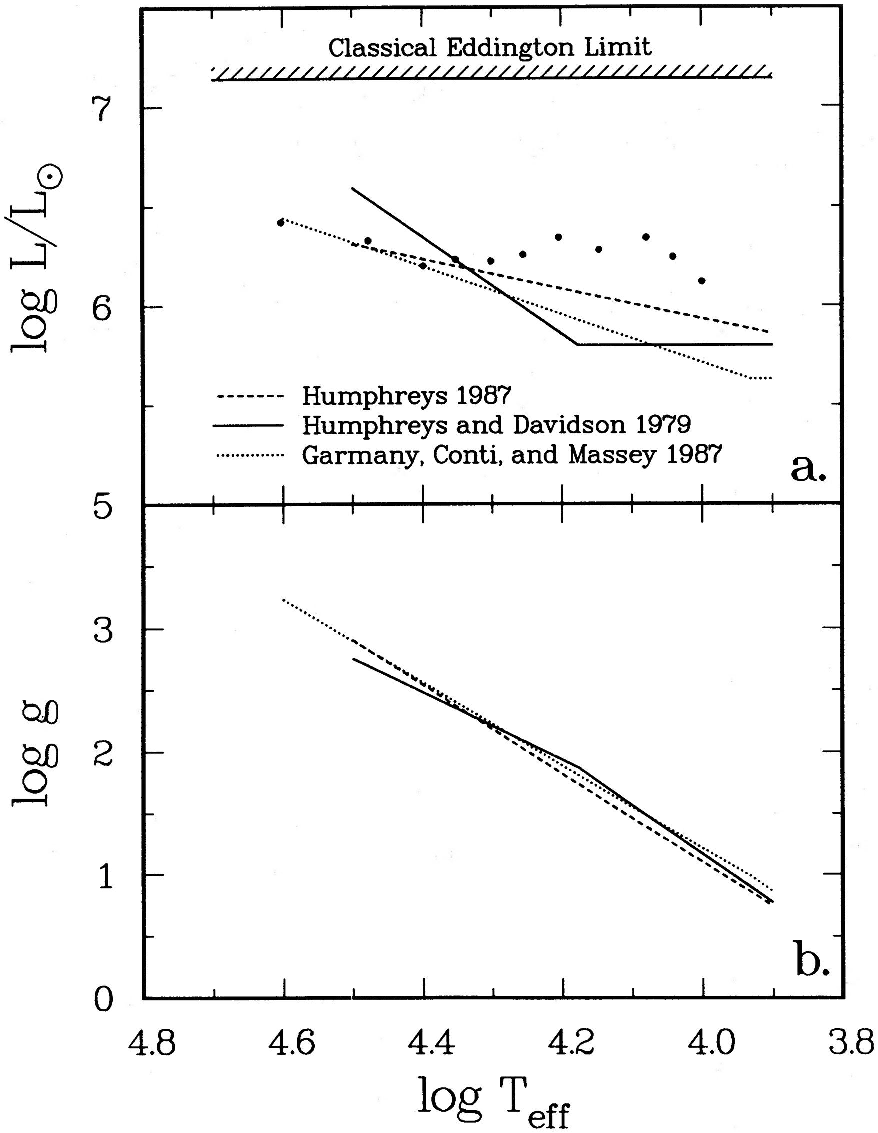

FIG. 1.—(*a*) Observed luminosity upper limits for Milky Way and LMC stars from Humphreys and Davidson (1979) (*solid line*), Garmany, Conti, and Massey (1987) (*dotted line*), and Humphreys (1987) (*dashed line*). The location of the classical Eddington limit for electron scattering is indicated. Filled circles indicate the locations of the true Eddington limit as determined from line blanketed model atmospheres (see § IV). (*b*) The observed luminosity limits are shown transformed into the log g–log T_{eff} plane, using the adopted mass-luminosity relation for the end of core hydrogen burning given in eq. (4) in the text.

TABLE 1

THE OBSERVED UPPER LUMINOSITY LIMITS[a]

	HUMPHREYS AND DAVIDSON 1979			GARMANY, CONTI, AND MASSEY 1987			HUMPHREYS 1987		
log T_{eff}	log $L/L_\odot$	log $M/M_\odot$	log g	log $L/L_\odot$	log $M/M_\odot$	log g	log $L/L_\odot$	log $M/M_\odot$	log g
4.6.........	6.82:	2.06:	3.03:	6.44	1.88	3.23	6.38:	1.85:	3.26:
4.5.........	6.59	1.95	2.75	6.32	1.83	2.89	6.31	1.82	2.90
4.4.........	6.36	1.85	2.47	6.20	1.77	2.56	6.23	1.78	2.54
4.3.........	6.12	1.73	2.20	6.08	1.71	2.22	6.16	1.75	2.18
4.2.........	5.89	1.62	1.92	5.95	1.65	1.89	6.08	1.71	1.82
4.1.........	5.80	1.58	1.57	5.83	1.60	1.55	6.01	1.68	1.46
4.0.........	5.80	1.58	1.17	5.71	1.54	1.22	5.93	1.64	1.10
3.9.........	5.80	1.58	0.77	5.63	1.50	0.86	5.86	1.61	0.74

[a] log $L/L_\odot$ values were computed from eqs. (1)–(3). Masses were derived from the mean mass-luminosity relation given in eq. (4). Values at log T_{eff} = 4.6 for Humphreys and Davidson 1979 and Humphreys 1987 are extrapolated.

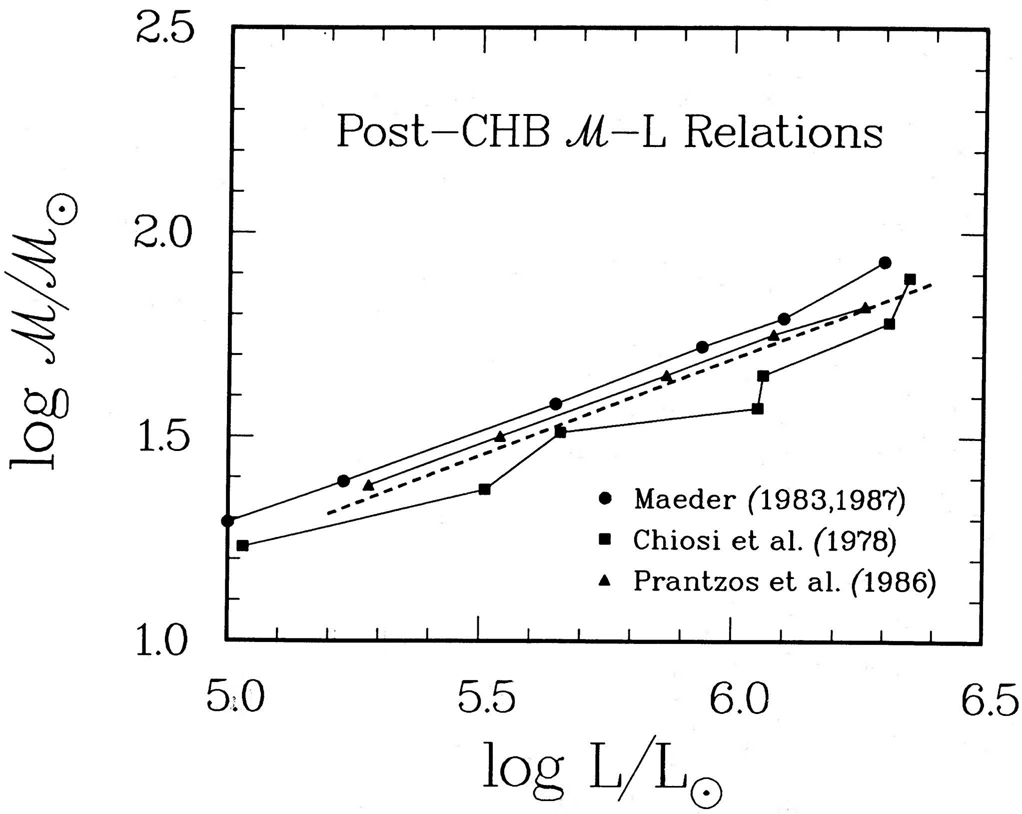

FIG. 2.—Mass-luminosity relations for the stellar evolution phase near the end of core hydrogen burning from the calculations of Maeder (1983, 1987) (*circles*), Chiosi *et al.* (1978) (*triangles*), and Prantzos *et al.* (1986) (*squares*). Dashed line shows a simple linear regression through the three sets of calculations over the range $\log L/L_\odot > 5.2$ and represents the mass-luminosity relation adopted in this paper. The equation of the line is given in eq. (4) in the text.

where κ_F is the flux-mean opacity (including electron scattering) and the rest of the symbols have their usual meanings. For the classical Eddington limit one adopts $\kappa_F = \sigma_E = 0.347$ for a fully ionized Population I gas.

The $T_{\rm eff}$-independent value of κ_F in the classical case produces a $T_{\rm eff}$-independent value of L_E for stars of a given mass. In reality, however, κ_F increases with decreasing $T_{\rm eff}$ in the range $10{,}000 \lesssim T_{\rm eff} \lesssim 30{,}000$ K due to the opacity of numerous metal lines in the Balmer continuum (see § V). In this temperature range the classical value of L_E overestimates the luminosity at which instability against radiation pressure sets in.

With a simple calculation, we can determine the effect of a $T_{\rm eff}$-dependent value of κ_F on the location of the Eddington limit in the HR diagram and in the $\log T_{\rm eff}$–$\log g$ diagram. First, we assume a mass-luminosity relation of the type

$$\log (L/L_\odot) = a + b \log (M/M_\odot) . \quad (6)$$

Next, for simplicity, we assume that the flux-mean opacity at $\tau_R \approx 1$ in the range of $10{,}000 \lesssim T_{\rm eff} \lesssim 30{,}000$ can be approximated by

$$\log \kappa_F = k - m \log (T_{\rm eff}/10^4) . \quad (7)$$

Then the location of the Eddington limit in the HR diagram is given by

$$\log (L_E/L_\odot) = a + [b/(b-1)](4.116 - a - k) + [mb/(b-1)] \log (T_{\rm eff}/10^4) \quad (8)$$

and in the $\log T_{\rm eff}$–$\log g$ diagram

$$\log g_E = (1.277 + k) + (4 - m) \log (T_{\rm eff}/10^4) . \quad (9)$$

A comparison between the observed luminosity upper limit and these predictions yields the dependence of κ_F on $T_{\rm eff}$ which would be required to explain the upper limit as the Eddington limit. If we adopt the upper limit of Garmany *et al.* (eq. [3a]) and the M-L relation of equation (4), we find that $k = -0.054$ and $m = 0.647$. This implies a flux-mean opacity of $\kappa_F = 0.36$ at $T_{\rm eff} = 40{,}000$ K, which is very close to the expected value of 0.35 for electron scattering, and $\kappa_F = 0.88$ at $T_{\rm eff} = 10{,}000$ K. This simple estimate shows that an increase in κ_F of about a factor of 2 between $T_{\rm eff} = 40{,}000$ K and 10,000 K is sufficient to explain the observed luminosity upper limit in terms of the Eddington limit.

b) The Eddington Limit in Model Atmospheres

An estimate of the location of the true Eddington limit can be obtained from model atmosphere calculations which include the full effects of metal line opacity, e.g., the models published by Kurucz (1979). In a study of the energy distributions of B-type supergiants in the Large Magellanic Cloud (Fitzpatrick 1987), we found that for many temperatures the lowest gravities included in Kurucz's grid of line-blanketed, LTE, plane-parallel models are too large to be representative of the supergiants and are often quite far from the radiation limit. We obtained the ATLAS model atmosphere program from Robert L. Kurucz and have extended his calculations (using solar abundances) to much lower gravities than were

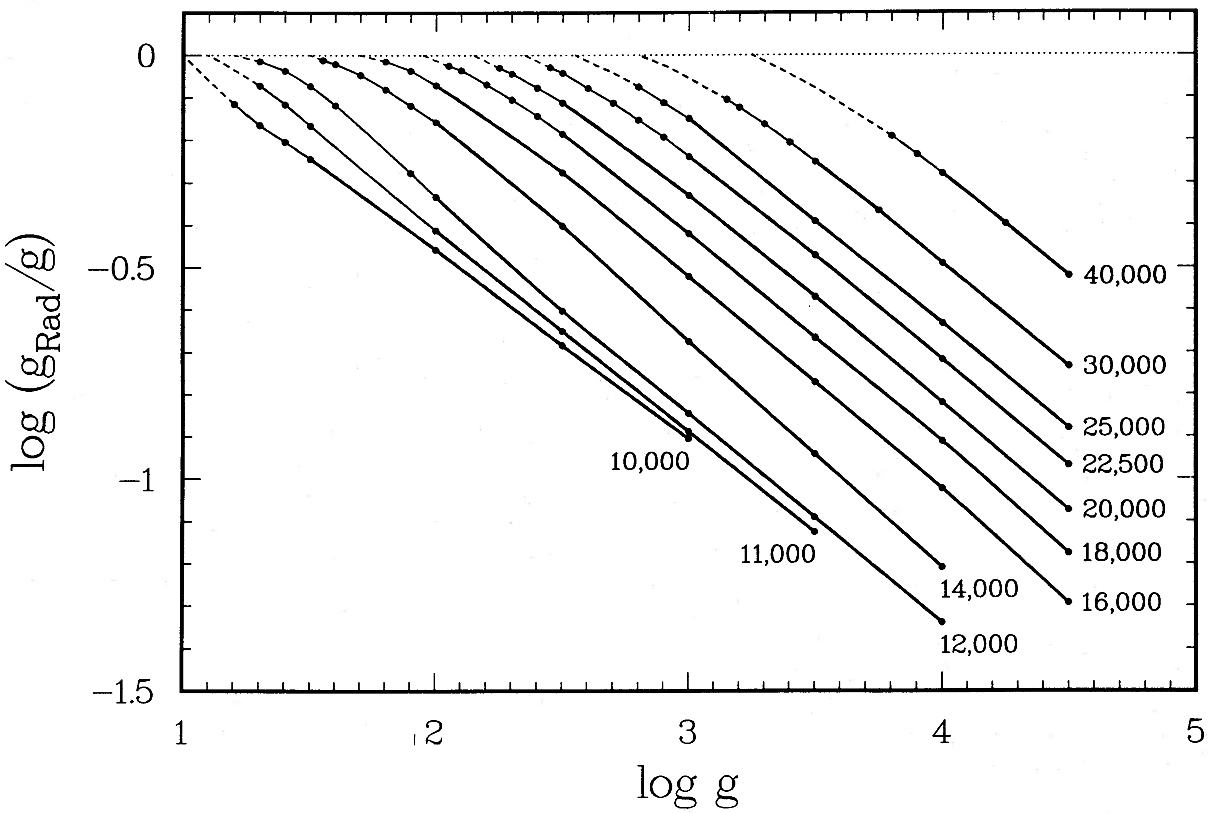

FIG. 3.—Log (g_{rad}/g) vs. log g for model atmospheres from the grid of Kurucz (1979) and from new calculations by the authors, using Kurucz's model atmosphere program. Individual models (*filled circles*) joined by the solid lines indicate sequences calculated at the effective temperatures given in the figure. The thick lines show the range of log g values for a given T_{eff} which appeared in Kurucz's published grid. The thin lines show the log g range of the newly calculated models. Dashed lines indicate our extrapolation to the Eddington limit for plane-parallel models, i.e., at log (g_{rad}/g) = 0 (*dotted line*). These Eddington limits are given in Table 2. The values of g_{rad} used in the figure are the maximum values found in the models in the optical depth range $10^{-2} \leq \tau_{Ross} \leq 10^2$.

included in the published grid. The properties of these low-gravity models are discussed in Fitzpatrick (1987). Here we simply utilize the results of the calculations and present our estimates of the true Eddington limits based on the line-blanketed models.

Figure 3 shows the log of the ratio of the radiative acceleration (g_{rad}) to the gravitational acceleration (the Newtonian gravity, g) plotted against log g for model calculations in the range $10{,}000 \leq T_{eff} \leq 40{,}000$ K. Individual models are represented by the filled circles. The condition of radiative instability occurs when the inward (gravitational) and outward (radiative) accelerations balance, i.e., log (g_{rad}/g) = 0 (dotted line in Fig. 3). The values of g_{rad} used in Figure 3 are the largest values found in the model atmospheres at optical depths $10^{-2} \leq \tau_{Ross} < 10^2$. The thick lines indicate the log g range (for a given T_{eff}) which appears in Kurucz's published grid of models. The thin lines indicate the range of low-gravity models we have calculated using Kurucz's atmosphere program. Our extrapolations to log (g_{rad}/g) = 0 are shown by the dashed lines, which thus indicate the locations of the true Eddington limits for line-blanketed, LTE, plane-parallel model atmospheres.

In Table 2 we list the log g values of the lowest gravity models calculated for each of the effective temperatures shown in Figure 3, along with the log g values of the estimated Eddington limits. For the models with $12{,}000 \leq T_{eff} \leq 22{,}500$ K the lowest gravity models are close to the instability point and the extrapolations are very secure. For the three hottest sets of models we used the shape of the log (g_{rad}/g) versus log g curve for the 22,500 K models to extrapolate to the Eddington limit. For the 10,000 and 11,000 K models the extrapolations were done by eye. Lower gravity models at these five effective temperatures could not be calculated because the surface point in the calculations ($\tau_{Ross} \approx 10^{-4.5}$) becomes unstable to radiation pressure and a static solution is not possible. This is not

TABLE 2

THE EDDINGTON LIMIT IN PLANE-PARALLEL MODEL ATMOSPHERES

T_{eff} (K)	log g_{min}[a]	log g_{Edd}[b]
40,000	3.70	3.25
30,000	3.15	2.80
25,000	2.80	2.55
22,500	2.45	2.35
20,000	2.25	2.15
18,000	2.05	1.95
16,000	1.80	1.70
14,000	1.55	1.50
12,000	1.30	1.20
11,000	1.30	1.10
10,000	1.20	1.00

[a] Lowest log g value for which a converged line-blanketed, LTE, plane-parallel model atmosphere was computed.

[b] Estimated log g value of the Eddington limit (see Fig. 3).

considered to be the true Eddington limit because the densities at these surface points are so low that such instabilities would add negligibly to the mass loss. In addition, in luminous stars considered to be stable, the tops of the photospheres merge with the stellar winds and are not static.

IV. THE EDDINGTON LIMIT AND THE OBSERVED UPPER LUMINOSITY LIMIT

In Figure 4 we compare the Eddington limits determined from the model atmosphere calculations (*filled circles*) with the upper luminosity limits given in § II. The shaded area shows the region within ± 0.1 dex in log g around the three luminosity relations shown in Figure 1*b*. This ± 0.1 dex margin represents the uncertainty in the log g values introduced by the transformation from luminosity to gravity, via the M-L relation.

The data show generally good agreement between the location of the Eddington limit and the observed luminosity limits, particularly for log $T_{\rm eff} \geq 4.3$. For temperatures in the range $4.0 \leq \log T_{\rm eff} \leq 4.3$ ($T_{\rm eff} = 10{,}000$–$20{,}000$ K) the model calculations allow slightly lower gravities than observed. However, this is the temperature-gravity range of the B-type supergiants, for which it is known that the opacities calculated by Kurucz underestimate the observed metal line opacity. This underestimate has two sources. First, B supergiants later than type B0.5 ($T_{\rm eff} < 20{,}000$ K) have extremely strong absorption by numerous lines of Fe III and other twice-ionized metals in the region around 2000 Å, which are not included in the model opacities (Swings *et al.* 1976; Castelli *et al.* 1980; Fitzpatrick 1987). These lines are located near the peaks of the energy distributions of the B supergiants. Second, Kurucz's opacity calculations assumed a microturbulence velocity of 2 km s^{-1}, while observations of B supergiants indicate that a value closer to 10 km s^{-1} is appropriate. An increase in the microturbulent velocity will cause a general enhancement in the metal line opacity. Castelli *et al.* (1980) have pointed out that the increase of the Fe III opacity and the increase of the microturbulence in B supergiants may explain the difference of a factor of 2 between the observed line blocking in the 2000 Å region and the values predicted by Kurucz's models. This underestimate of the metal line opacity in the Kurucz's models for B supergiants implies that the gravities of the models at the Eddington limits are also underestimated. An increase in the flux-mean opacity by $\sim$40% for the models with $10{,}000 \lesssim T_{\rm eff} \lesssim 20{,}000$ K would bring the minimum gravity of the calculated models into the range of gravities of the stars at the observed luminosity limit.

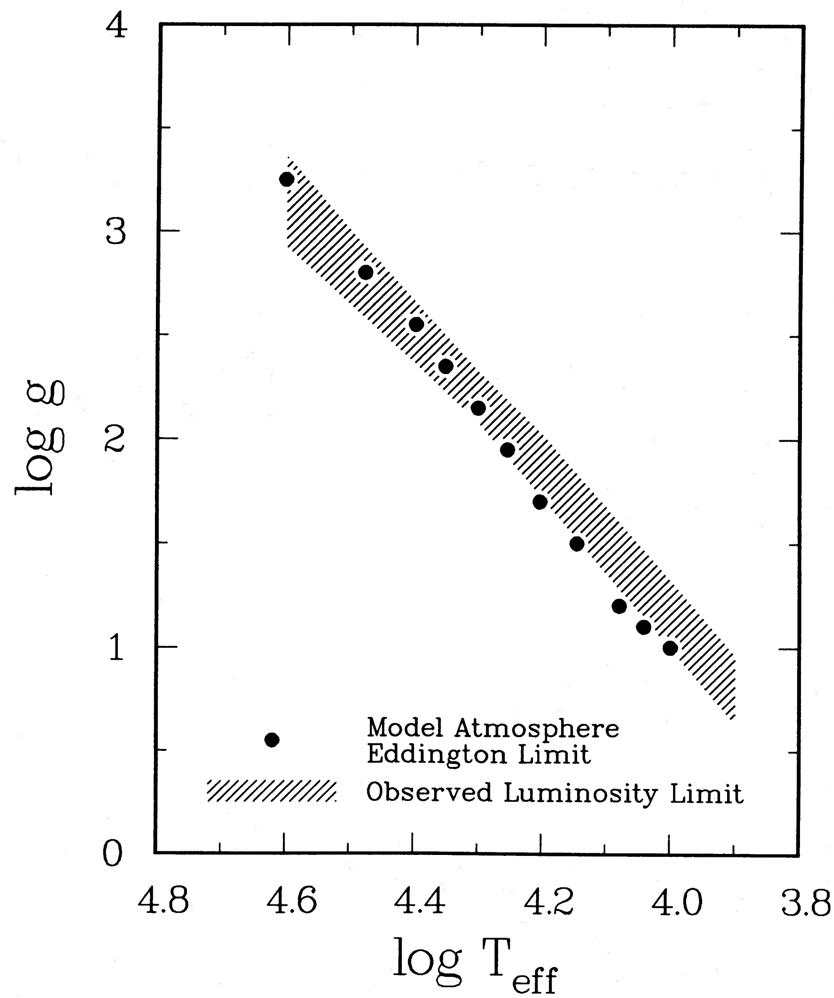

FIG. 4.—Comparison of model atmosphere Eddington limits (*filled circles*) with the observed luminosity upper limits. Hatched area indicates the region within ± 0.1 in log g of the observed limits shown in Fig. 1*b*.

In Figure 1*a* we also show the model atmosphere Eddington limits transformed into the log $T_{\rm eff}$–log L plane (*filled circles*). A hump in the Eddington luminosities centered near log $T_{\rm eff} = 4.15$, which we believe is the signature of the opacity underestimation, is clearly visible. With the adopted M-L relation, luminosity is proportional to $g^{1.9}$, thus discrepancies between the predicted and observed gravities are magnified when comparing luminosities.

Kurucz (1987 and private communication) plans to recompute the metal line opacities, including both an increased number of Fe III lines and various microturbulence velocities. These calculations will allow us to refine the location of the Eddington limits for temperatures in the range 10,000–20,000 K. The Eddington limits in this range will certainly shift to larger gravities and lower luminosities, and thus into better agreement with the observations.

We conclude that the observed $T_{\rm eff}$-dependent luminosity limit in the range $4.0 \leq \log T_{\rm eff} \leq 4.6$ coincides with the Eddington limit given by *plane-parallel* model atmospheres when the known shortcomings in the opacities are taken into account. The interpretation of this result is not completely straightforward because the plane-parallel assumption is certainly incorrect for stars with very low gravities. As the Newtonian gravity decreases, a stellar atmosphere is expected to become increasingly extended. This suggests that the "Eddington limits" as estimated from the plane-parallel models do not necessarily indicate the log g values at which real stellar photospheres become unstable against radiation pressure. Rather, these "Eddington limits" should be regarded as indicating the log g values at which the photospheres have Γ values very close to one, where $\Gamma \equiv 1 - g_{\rm rad}/g$, and are very tenuously bound.

Given the above discussion, our interpretation of our results is as follows. As stars with initial masses greater than $\sim 40\ M_\odot$ evolve toward the HD limit, their effective gravities decrease ($\Gamma + 1$). Simple radiation driven wind theory (Castor, Abbott, and Klein 1975) predicts that mass-loss rates should scale inversely with some power of the effective gravity. Thus the mass-loss rates should increase substantially as evolution approaches the HD limit. At some point the effective gravities have decreased enough, and the mass-loss rates increased enough, that further redward evolution is halted. These critical values of the effective gravities correspond to the observed luminosity limit and occur at log g values close to the "Eddington limits" predicted from plane-parallel models. As noted in § I, stars with large mass-loss rates are indeed observed near the upper luminosity limits. In addition, the properties of the LBV's are consistent with this scenario (see § VI).

V. THE UPPER LUMINOSITY LIMIT FOR YELLOW AND RED SUPERGIANTS

The $T_{\rm eff}$-*independent* part of the observed upper luminosity limit, i.e., $\log (L/L_\odot)_{\rm max} \approx 5.7$ for $T_{\rm eff} < 6000$–15,000 K, can also be understood as a consequence of metal line opacity in the stellar atmospheres. Lamers (1987) has shown that, at a given density, the value of κ_F increases with decreasing temperature in the range $10{,}000 \leq T_{\rm eff} \leq 40{,}000$ K, reaches a maximum in the range $8000 \leq T_{\rm eff} \leq 10{,}000$ K (depending on the density) and thereafter decreases with decreasing $T_{\rm eff}$. The presence of a maximum in $\kappa_F(T_{\rm eff})$ implies that stars below a certain minimum luminosity, $L_{\rm crit}$, will not encounter the Eddington limit during their expansion to the red supergiant phase. This is due to the fact that the gravity varies as $g \propto R^{-2} \propto T_{\rm eff}^4$ when a massive star moves to the red in the HR diagram, whereas the radiation pressure varies as $g_{\rm rad} \propto \kappa_F T_{\rm eff}^4$. So, if a star in its redward evolution does not become unstable against radiation pressure when $\kappa_F(T_{\rm eff})$ reaches its maximum (i.e., near $T_{\rm eff} \approx 8000$–10,000 K), it will not be unstable when it subsequently evolves (at $\sim$constant L) to lower temperatures, despite the fact that g decreases proportionally with $T_{\rm eff}^4$.

The "kink" in the upper luminosity limit is thus expected to occur at the temperature where κ_F reaches its maximum value ($\sim$8000–10,000 K) and the expected luminosity upper limit for yellow and red supergiants is thus equal to the Eddington limit at the same temperature.

VI. THE EDDINGTON LIMIT AND THE LUMINOUS BLUE VARIABLES

During quiescence, the LBVs co-exist in the HR diagram with normal supergiants in a band of width $\Delta \log T_{\rm eff} \approx 0.3$, located just *to the left* of the upper luminosity limit (e.g., de Jager 1980, p. 10; Lamers 1986*a*). Their quiescent mass-loss rates are a factor of 3–10 higher than for normal supergiants, indicating that LBVs are more unstable than normal supergiants of similar L and $T_{\rm eff}$, despite their general location to the left of the luminosity upper limit. This instability of the LBVs and their location in the HR diagram can be explained in a natural way by the changing position of the Eddington limit in the HR diagram when the stars evolve with a high mass-loss rates.

Evolutionary calculations have shown that the luminosity of massive stars remains approximately constant after the CHB phase even if the stars lose a considerable amount of matter (see § II*b* and the references therein). By combining this constant luminosity evolution scenario with equations (5) and (7) we can describe the change in the position of the Eddington limit for an evolving, mass-losing star. If a star with a given luminosity L and mass $M(0)$ after the CHB phase reaches its Eddington limit at an effective temperature $T_{\rm E}(0)$, then the Eddington limit will shift to higher effective temperatures $T_{\rm E}(t)$, as the mass $M(t)$ decreases with time and the luminosity remains constant, by an amount

$$\log T_{\rm E}(t) = \log T_{\rm E}(0) - m^{-1} \log [M(t)/M(0)] \ . \qquad (10)$$

Assuming $m \approx 0.65$ (§ III*a*) we find that $T_{\rm E}$ increases by a factor of 1.7 if the mass decreases by a factor 0.7. This implies that a star which has reached the upper luminosity limit and starts to lose a considerable amount of mass can only find stability against radiation pressure if it moves back toward higher temperatures as its mass decreases (because the flux mean opacity decreases with increasing temperature).

Evolution calculations by Maeder (1983, 1987) and Prantzos *et al.* (1986) have shown that the definitive leftward motion in the HR diagram for massive stars starts when the stars have about half of their initial mass. Since the stars have lost, at most, 25% of their initial mass when they first reach the upper luminosity limit, they can lose more than 25% of their initial mass as a B-type supergiant or LBV. This simple estimate shows that the ratio $M(t)/M(0)$ in equation (10) can become as small as $\frac{2}{3}$, which would imply a maximum shift of the instability limit of $\Delta \log T_{\rm eff} \approx 0.3$ to the left of the upper luminosity limit, which is consistent with the observed location of the LBVs.

We suggest that the conflict between the natural tendency of the stars to move to the right in the HR diagram by expansion after the CHB phase and the leftward motion of the stability limit results in a large increase in the mass loss rates and in the violent outbursts of the LBVs (see Lamers 1986*a*, 1987; Davidson 1987*a*, *b*). The stars will become more and more unstable with time, since the mass and the gravity decrease due to the enhanced mass loss but the luminosity remains the same. This instability phase will end when the star has lost so much mass that it starts to evolve to the left and becomes a W-R star. This suggestion implies that the LBVs are older than the more normal supergiants which are found in the same part of the HR diagram and that the LBVs have already lost more mass. This is consistent with observations that several LBVs clearly show an overabundance of N and an underabundance of C and O (e.g., Lamers 1986*a*; Davidson *et al.* 1986). This is a characteristic property of post–CHB stars which have already lost a large fraction of their mass.

There is also theoretical support for the suggestion that the high mass-loss rates of the LBVs and their outbursts are due to radiation pressure near the Eddington limit. Lamers (1986*b*) has shown that the outflow velocity of the star P Cygni during quiescence can be explained by radiation pressure produced by metal-line absorptions of a large fraction of the stellar luminosity. Appenzeller (1986) has argued that the outbursts of the LBVs and the resulting excursions to the right in the HR diagram can be explained only by radiation pressure due to metal lines.

VII. DISCUSSION

In this paper we have compared the observed upper luminosity limit for massive stars, expressed in a log T_{eff}–log g diagram, with the location of the plane-parallel LTE model atmospheres which become unstable against radiation pressure. The good agreement between the predicted and observed limits strongly suggests that the observed luminosity limit is due to high mass loss produced by a large reduction in the effective gravity in the stellar atmosphere due to radiation pressure.

The luminosity limit for stability of stellar atmospheres against radiation pressure, which we called the Eddington limit, is different from the classical Eddington limit in a fundamental way. In the classical limit, the star is unstable against radiation pressure due to electron scattering. This implies that all the layers of the envelope above the energy generating core are unstable: the star cannot exist. However, in our calculations of the Eddington limit for model atmospheres, the radiative force dominates the gravity only in the photosphere; the deeper layers at $\tau_R > 1$ are stable. This is due to the fact that the radiation pressure produced by the spectral lines becomes efficient only at optical depths $\tau_R \lesssim 1$. In the deeper layers where $\tau_R \gg 1$, the radiation field satisfies the diffusion approximation which implies that $F_\nu \approx \kappa_\nu^{-1}$, and so the radiative force $F_\nu \kappa_\nu/c$ produced by a spectral line at frequency ν is the same as that of the neighboring continuum. Therefore, a star which expands after the CHB phase and reaches our calculated Eddington limit will suffer a high mass loss from the photosphere but will not be disrupted completely.

De Jager (1980, 1984) has suggested that the observed luminosity limit is due to high mass loss in the atmosphere produced by a turbulent pressure. Turbulent pressure may indeed reduce the effective gravity in the stellar atmospheres and facilitate the mass loss, as shown by de Jager. However, there are three arguments which suggest that radiation pressure is the dominant mechanism: (*a*) The calculated radiation pressure in model atmospheres produces a good agreement between the predicted and the observed luminosity limits. (*b*) The velocity law in the lower part of the wind of P Cygni at $R_* \lesssim r \lesssim 4\,R_*$ cannot be explained by turbulent pressure, but only by radiation pressure (Lamers 1986*b*). (*c*) The "turbulent velocities," determined from the studies of the equivalent widths of photospheric lines of stars near the luminosity limit contain a nonnegligible contribution from differential velocities produced by outflow in the line-forming region. For instance, in the atmosphere of a typical late-B supergiant near the HD limit ($\log L/L_\odot = 5.8$; $T_{\mathrm{eff}} = 12{,}000$ K, $R = 185\,R_\odot$ and $M = 39\,M_\odot$) with a mass-loss rate of $10^{-5}\,M_\odot\,\mathrm{yr}^{-1}$ and a density structure derived from an LTE model atmosphere, the outflow velocity increases from 1.2 km s^{-1} at $\tau_R = 10^{-1}$ to 23 km s^{-1} at $\tau_R = 10^{-2.5}$. Such a differential velocity will mimic "microturbulence" in the formation of the lines. Therefore, at least part of the relation between the "observed microturbulence" and the turbulence required to explain the high mass-loss rates of stars near the HD-limit, derived by de Jager (1984), may be due to differential velocities in atmospheres which are unstable against radiation pressure.

Maeder (1983) has suggested that the periodic large outbursts of the LBVs are due to the fact that they repeatedly run into the de Jager limit (the limit of stability against turbulent pressure). Each time they pass this limit during their expansion, a considerable amount of mass is ejected, typically 10^{-3} to $10^{-1}\,M_\odot$, which moves the star in the HR diagram back to the left of the de Jager limit. The subsequent continued expansion will bring the star again to the de Jager limit. In our interpretation of the LBVs, in which the instability is due to radiation pressure, the same scenario can be expected to occur.

Finally, we note that the location of the observed luminosity limit has been used in some stellar evolution studies to determine the magnitude of convective overshooting in the cores of massive stars (e.g., Doom 1982). In these studies, "normal" mass-loss rates were assumed throughout the evolution and an overshooting parameter was explicitly adjusted to reproduce the observed maximum luminosity for late-type supergiants. Our results indicate that such a procedure is not correct, because the mass-loss rates of stars approaching the luminosity limit will increase substantially. While enhanced mixing is undoubtedly present in the interiors of massive stars, to clearly separate its effects on the HR diagram from those of mass loss will require a detailed physical understanding of both processes.

The authors gratefully acknowledge P. Conti, C. de Loore, C. de Jager, R. Humphreys, and K. Davidson for comments and suggestions on this paper and R. Kurucz for providing a copy of his ATLAS model atmosphere program. H. J. G. L. M. L. thanks the staff of JILA and CASA for hospitality during the autumn of 1986 when this paper was written. This work was supported in part by National Science Foundation grant AST 85-20728 and NASA grant NSG-5300 to the University of Colorado.

REFERENCES

Appenzeller, I. 1986, in *Luminous Stars and Associations in Galaxies*, ed. C. de Loore, P. Laskarides, and A. Willis (Dordrecht: Reidel), p. 139.
Castelli, F., Lamers, H. J. G. L. M., Llorente de Andrés, F., and Müller, E. A. 1980, *Astr. Ap.*, **91**, 32.
Castor, J. I., Abbott, D. C., and Klein, R. I. 1975, *Ap. J.*, **195**, 157.
Chiosi, C., Nasi, E., and Sreenivasan, S. R. 1978, *Astr. Ap.*, **63**, 103.
Conti, P. S. 1984, in *IAU Symposium 105, Observational Tests of the Stellar Evolution Theory*, ed. A. Maeder and A. Renzini (Dordrecht: Reidel), p. 233.
Davidson, K. 1987*a*, in *Instabilities in Luminous Early-Type Stars*, ed. C. de Loore and H. J. G. L. M. Lamers (Dordrecht: Reidel), in press.
———. 1987*b*, *Ap. J.*, in press.
Davidson, K., Dufour, R. J., Walborn, N. R., and Gull, T. R. 1986, *Ap. J.*, **305**, 867.
de Jager, C. 1980, *The Brightest Stars*, (Dordrecht: Reidel).
———. 1984, *Astr. Ap.*, **138**, 246.
Doom, C. 1982, *Astr. Ap.*, **116**, 308.
Fitzpatrick, E. L. 1987, *Ap. J.*, **312**, 596.
Garmany, C. D., Conti, P. S., and Massey, P. 1987, *A.J.*, in press.
Humphreys, R. 1987, in *Instabilities in Luminous Early-Type Stars*, ed. C. de Loore and H. J. G. L. M. Lamers (Dordrecht: Reidel), in press.
Humphreys, R., and Davidson, K. 1979, *Ap. J.*, **232**, 409.
———. 1984, *Science*, **223**, 243.
Kurucz, R. L. 1979, *Ap. J. Suppl.*, **40**, 1.
———. 1987, in *Proc. of the IAU General Assembly*, New Delhi (in press).
Lamers, H. J. G. L. M. 1986*a*, in *Luminous Stars and Associations in Galaxies*, ed. C. de Loore, P. Laskarides, and A. Willis (Dordrecht: Reidel), p. 157.
———. 1986*b*, *Astr. Ap.*, **159**, 90.
———. 1987, in *Instabilities in Luminous Early-Type Stars*, ed. C. de Loore and H. J. G. L. M. Lamers (Dordrecht: Reidel), in press.
Maeder, A. 1982, *Astr. Ap.*, **105**, 149.
———. 1983, *Astr. Ap.*, **120**, 113.
———. 1987, *Astr. Ap.*, **173**, 247.
Prantzos, N., Doom, C., Arnould, M., and de Loove, C. 1986, *Ap. J.*, **304**, 695.
Pylyser, E., Doom, C., and de Loore, C. 1985, *Astr. Ap.*, **148**, 379.
Swings, J. P., Klutz, M., Vreux, J. M., and Peytremann, E. 1976, *Astr. Ap. Suppl.*, **25**, 193.
Wolf, B., Appenzeller, I., and Cassatella, A. 1980, *Astr. Ap.*, **88**, 15.

EDWARD L. FITZPATRICK: Joint Institute for Laboratory Astrophysics, University of Colorado, Boulder, CO 80309-0440

HENNY J. G. L. M. LAMERS: SRON Laboratory for Space Research, Beneluxlaan 21, NL-3527 HS Utrecht, The Netherlands